Life Sciences 218 (2019) 31–37

Contents lists available at ScienceDirect

Life Sciences

journal homepage: www.elsevier.com/locate/lifescie

MiR-219 represses expression of *dFMR1* in *Drosophila melanogaster*

Chao Wang[a,b], Liang Ge[a], Jianban Wu[a], Xuan Wang[a], Liudi Yuan[a,c,*]

[a] Key Laboratory of Developmental Genes and Human Disease, Ministry of Education, Institute of Life Sciences, Southeast University, Nanjing 210096, China
[b] State Key Laboratory for Pharmaceutical Biotechnology, Nanjing University, Nanjing 210023, China
[c] School of Medicine, Southeast University, Nanjing 210009, China

ARTICLE INFO

Keywords:
Drosophila
dFMR1
Screening
miR-219
NMJ

ABSTRACT

Aims: Fragile X mental retardation protein (FMRP) plays a vital role in mRNA trafficking and translation inhibition to regulate the synthesis of local proteins in neuronal axons and dendritic terminals. However, there are no reports on microRNA (miRNA)-mediated regulation of FMRP levels in *Drosophila*. Here, we aimed to identify miRNAs regulating FMRP levels in *Drosophila*.

Main methods: Using online software, we predicted and selected 11 miRNAs potentially acting on the *Drosophila* fragile X mental retardation 1 (*dFMR1*) transcript. These candidates were screened for modulation of *dFMR1* transcript levels at the cellular level using a dual luciferase reporter system. In addition, we constructed a transgenic *Drosophila* model overexpressing miR-219 in the nervous system and quantified dFMRP by western blotting. The neuromuscular junction phenotype in the model was studied by immunofluorescence staining.

Key findings: Among the 11 miRNAs screened, miR-219 and miR-960 reduced luciferase gene activity by binding to the 3′-UTR of the *dFMR1* transcript. Mutation of the miR-219 or miR-960 binding sites on the transcript resulted in complete or partial elimination of the miRNA-induced repression. Western blots revealed that dFMRP expression was decreased in the miR-219 overexpression model (Elav > miR-219). *Drosophila* larvae overexpressing miR-219 showed morphological abnormalities at the neuromuscular junction (increased synaptic boutons and synaptic branches). This finding is consistent with some phenotypes observed in *dfmr1* mutants.

Significance: Our results suggest that miR-219 regulates *dFMR1* expression in *Drosophila* and is involved in fragile X syndrome pathogenesis. Collectively, these findings expand the current understanding of miRNA-mediated regulation of target molecule-related functions.

1. Introduction

Fragile X mental retardation protein (FMRP), coded by *fragile X mental retardation 1* (*FMR1*) [1], is most commonly found in the brain and is essential for proper cognitive development and female reproductive function. Mutations of *FMR1* can lead to fragile X syndrome [2], intellectual disability [3], premature ovarian failure [4,5], autism [6,7], Parkinson's disease [8], developmental delays [9] and other cognitive deficits [9]. FMRP is an RNA-binding protein that binds to specific mRNAs and related proteins [10]. It functions as a negative regulator and represses the translation of target mRNAs, but loses its repression effect when mutated [11].

FMRP has different functions, including regulating nerve development and synaptic plasticity in different areas of the nervous system. Specifically, in neurons, FMRP is thought to shuttle between the nucleus and cytoplasm, thus facilitating nuclear export of mRNAs to dendrites and the synthesis of synaptic proteins [12]. Observing the influence of FMRP deficiency on neurons by studying fragile X syndrome may improve our understanding of the function of FMRP. A study in a mouse model of fragile X mental retardation revealed that FMRP participates in synaptic plasticity, which requires de novo generation of proteins that respond to the stimulation of activated synaptic receptors, thereby inducing changes in glutamate receptor-mediated long-term depression [13]. This finding links synaptic plasticity and synaptic connection changes with the dynamic processes of learning and memory.

It has been shown that FMRP mediates RNA interference and participates in microRNA (miRNA) pathways to inhibit the translation of target mRNAs by binding to Argonaute 2 (AGO2) and RNA-induced silencing complexes (RISCs), or by regulating the level of miRNA

Abbreviations: FMRP, fragile X mental retardation protein; FMR1, fragile X mental retardation 1; dFMR1, *Drosophila* fragile X mental retardation 1; miRNA, micro ribonucleic acid; PBS, phosphate-buffered saline; NMJ, neuromuscular junction; HRP, horseradish peroxidase; DLG, discs large

* Corresponding author at: School of Medicine, Southeast University, 87 Dingjiaqiao Road, Nanjing 210009, China.
E-mail address: yld@seu.edu.cn (L. Yuan).

https://doi.org/10.1016/j.lfs.2018.12.008
Received 16 August 2018; Received in revised form 27 November 2018; Accepted 5 December 2018
Available online 05 December 2018

[14–16]. It has been suggested that miRNAs can also inhibit the transcription of *FMR1* in the neurons when FMRP expression in the brain is high by acting on the 3′-UTR of the *FMR1* gene, without affecting its protein level [17].

The first *FMR1* homologue in invertebrates was isolated from *Drosophila*, which has only one *FMR1* homologue (*dFMR1*). dFMRP has a high degree of amino acid sequence homology to FMRP in vertebrates and shows remarkably similar functions [18]. As mentioned above, FMRP interacts with miRNA regulatory pathways; some miRNAs are regulated by FMRP, and FMRP and miRNAs can work together to repress the translation of target mRNAs. However, studies on miRNAs regulating dFMRP in *Drosophila* are rarely reported.

2. Materials and methods

2.1. Vectors, bacterial strain, cell line, and animals

pAc5.1/V5-HisA, pP{UAST}, pGL3-Basic, and pRL vectors were from lab stock. *Escherichia coli* strain DH5α was used for cloning. The *Drosophila* cell line Kc167 was bought from Biovector Science Lab. Inc. (Beijing, China). Wild-type fly w^{1118} and nervous system GAL4 driver fly elav-Gal4 were stocked by our lab. The *dfmr1* mutant line BL6930 was obtained from Bloomington Drosophila Stock Center (Indiana University, Bloomington, IN, USA).

2.2. Sequences and bioinformatics analysis

All reference sequences, including miRNAs, their precursors, *dFMR1* coding sequence, and its 3′-UTR were obtained from Flybase (http://flybase.org/). We employed three online predicting programmes, miRanda (http://www.microrna.org/), TargetScan (http://www.targetscan.org) and PicTar (https://pictar.mdc-berlin.de/), to predict potential miRNAs targeting the *dFMR1* transcript. miRanda searches for complementarity matches between miRNAs and 3′-UTRs using dynamic programming alignment and thermodynamic calculation. Candidate miRNAs were post-processed, first by filtering out the miRNAs not consistently conserved according to target sequence similarity with *D. pseudoobscura* and *A. gambiae* and finally, by sorting and ranking all remaining candidates [19]. TargetScan combines thermodynamics-based modelling of RNA:RNA duplex interactions with comparative sequence analysis to predict miRNA targets conserved across multiple genomes [20]. PicTar scores common targets of several microRNAs and allows the identification of targets for both single microRNAs and combinations of microRNAs [21]. Our strategy consisted in the combination of multiple software to draw upon the strength of each programme to offset the shortcomings of every single software, so that the most likely miRNAs targeting the 3′-UTR of the *dFMR1* mRNA could be identified. In this way, potential combinations of miRNAs and targeted mRNAs may have been missed; however, we could vastly reduce the number of potential combinations for subsequent experiments.

2.3. Recombinant plasmid generation

The luciferase coding sequence from pGL3-Basic was subcloned into pAc5.1/V5-HisA to generate pAc-luc. The 3′-UTR sequence of the *dFMR1* transcript was inserted immediately after the luciferase coding sequence to generate pAc-luc-*dFMR1*UTR, which was used to express the luciferase reporter. All 11 potential miRNA precursors identified were amplified by polymerase chain reaction (PCR) and cloned into pAc5.1/V5-HisA vector to generate pAc-miR-1010, pAc-miR-219, pAc-miR-277, pAc-miR-281, pAc-miR-960, pAc-miR-974, pAc-miR-976, pAc-miR-1007, pAc-miR-1017, pAc-miR-991, and pAc-miR-375. These vectors were used to express the potential miRNAs in cells. In addition, we constructed two mutants of pAc-luc-*dFRM1*UTR named pAc-luc-*dFMR1*UTR_mut1 and pAc-luc-*dFMR1*UTR_mut2. In pAc-luc-*dFMR1*UTR_mut1, both targeting sites (506–512 and 1346–1352 nt of the 3′-UTR of *dFMR1* transcript) of miR-219 were replaced with restriction sites. In pAc-luc-*dFMR1*UTR_mut2, the single binding site (1286–1292 nt of the 3′-UTR of *dFMR1* transcript) of miR-960 was replaced with a restriction site.

2.4. Cell culture and transient transfection

D. melanogaster Kc167 cells were grown in Schneiders Drosophila medium (Gibco/Invitrogen, Carlsbad, CA, USA) with 10% foetal bovine serum (Gibco) at 25 °C. Cells (2×10^6 cells/well) were seeded in 12-well plates (Corning, NY, USA) and cultured for 24 h. In each well, 2 μg miRNA expression plasmid, 0.5 μg pAc-luc-*dFMR1*UTR (or pAc-luc-*dFMR1*UTR_mut1/2), and 0.1 μg pRL were co-transfected into cells by using FuGENE® HD Transfection Reagent (Roche, Mannheim, Germany) according to manufacturer's instructions. The Renilla luciferase expressed by pRL was used as an internal reference.

2.5. Luciferase activity determination

After 36 h of transient transfection, the suspended cells were pelleted by centrifugation at 2000 rpm for 5 min. The cell pellets were washed twice with phosphate-buffered saline (PBS) and the cells were lysed with 100 μl of cell lysis buffer by freeze-thawing at −70 °C once. The cell residues were removed by centrifugation (12,000 rpm, 10 min, 4 °C), and the supernatant was transferred to a new centrifuge tube. Ten microlitres of the supernatant was added to 20 μl of firefly luciferase substrate, mixed, and placed in a Turner Biosystems 20/20^n luminometer (Thermo Fisher Scientific, Waltham, MA, USA) for measurement. Next, 20 μl of Renilla luciferase substrate was added, mixed, and the values and ratios were recorded.

2.6. UAS-mir-219 transgenic line generation

A portion of the mir-219 locus (predicted 809-bp pri-mir-219) was subcloned from the wild-type genome into the *Xho*I and *Xba*I restriction sites of the pP{UAST} vector to generate the UAS-mir-219 construct. The primers used to amplify the mir-219 region were: primer1_miR-219 5′-ATC TCG AGC TGA CAG GCT CCC TAC TAA AC-3′ and primer2_miR-219 5′-CGT CTA GAT TTA AGG CAG CAG TAC GAT G-3′. The UAS-mir-219 construct was microinjected into wild-type embryos to generate transgenic flies using a standard germ-line transformation method [22,23].

2.7. Western blotting

Western blotting was conducted according to standard procedures [24] using mouse monoclonal antibodies against FMRP (Developmental Studies Hybridoma Bank, Iowa City, IA, USA) and α-tubulin (Sigma-Aldrich, St. Louis, MO, USA). Horseradish peroxidase (HRP)-conjugated goat anti-mouse IgG (Jackson ImmunoResearch Inc., West Grove, PA, USA) was used as a secondary antibody at a dilution of 1:5000.

2.8. Immunohistochemistry

Third-instar larvae were dissected to collect neuromuscular junctions (NMJs) according to a previously published procedure [25]. NMJs were treated with 4% paraformaldehyde in PBS for 40 min, then rinsed with 0.3% Triton X-100 in PBS. Primary antibodies used for immunohistochemistry included anti-discs large (anti-DLG, 1:500, Developmental Studies Hybridoma Bank) and anti-HRP (1:50, Jackson ImmunoResearch Inc.). Diluted (1:1000) secondary antibodies (Bioworld Technology, Louis Park, MN, USA) conjugated to tetramethylrhodamine (TRITC) or fluorescein isothiocyanate (FITC) were reacted for 2 h at room temperature. NMJ quantification was conducted largely following a previously described procedure [25]. All images were three-dimensional projections from complete z-stacks through the

entire NMJ of an abdominal segment. Synaptic boutons were defined on the basis of anti-HRP (presynaptic marker) and anti-DLG (postsynaptic marker) staining in merged images. ImageJ (National Institutes of Health, Bethesda, MD, USA) was used to quantify fluorescence intensities. Branch was defined as an axonal projection with at least two synaptic boutons. Branch, bouton, and mini-bouton numbers were counted for each NMJ.

2.9. Statistical analysis

All data were expressed as the mean ± standard deviation (SD). The data were tested for normality (IBM SPSS Statistics Version 19.0, Inc., Chicago, IL, USA) before being analysed using either parametric analysis of variance (ANOVA) or non-parametric tests. Western blot data were analysed using non-parametric Mann-Whitney tests (two-tailed, 95% CI) in GraphPad Prism Version 6.0 (GraphPad Software, Inc., San Diego, CA, USA). Morphological quantification data were analysed by non-parametric Kruskal-Wallis tests (two-tailed, 95% CI) and post-hoc tests (Dunn's multiple comparisons test) in GraphPad Prism. The criterion for statistical significance was set at $P < 0.05$.

3. Results

3.1. Prediction of miRNAs that can act on the transcript of dFMR1

We used three software (miRanda, TargetScan, and PicTar) to predict miRNAs that potentially act on the 3′-UTR of the *dFMR1* transcript. In total, 11 miRNAs were selected for subsequent experiments (Table 1) either because two or all three software predicted them, or because they were predicted with a high score by one software.

3.2. Screening of candidate miRNAs acting on the 3′-UTR of dFMR1 transcript in Kc167 cells

To observe the effect of different miRNAs on the reduction of luciferase expression when they act on the 3′-UTR of the *dFMR1* transcript, three plasmids, including the vector expressing the candidate miRNA (or empty plasmid), the vector expressing the tandem structure of luciferase and 3′-UTR of the *dFMR1* transcript, and the vector expressing Renilla luciferase as an internal reference, were co-transfected into Kc167 cells. The values of luciferase activity relative to the blank control (empty pAc5.1 plasmid, $n = 14$) were 97.00 ± 16.10, 61.21 ± 16.61, 141.18 ± 32.59, 103.06 ± 16.85, 112.94 ± 39.48, 92.75 ± 14.85, 80.92 ± 15.32, 74.63 ± 25.01, 91.24 ± 20.42, 82.62 ± 15.73, 72.81 ± 5.27, 77.47 ± 15.25, and 71.91 ± 15.85% when miR-274 (negative control, $n = 14$), miR-315 (positive control, $n = 14$), miR-281 ($n = 5$), miR-1007 ($n = 5$), miR-1017 ($n = 5$), miR-1010 ($n = 4$), miR-976 ($n = 5$), miR-991 (n = 5), miR-277 ($n = 6$), miR-375 ($n = 5$), miR-974 ($n = 4$), miR-219 ($n = 7$), and miR-960 ($n = 8$), respectively, were expressed (Fig. 1A). We selected miR-219 and miR-960, two miRNAs with the strong luciferase activity-reducing effect, for further analysis.

Table 1
MiRNAs predicted to interact with the 3′-UTR of the dFMR1 transcript.

miRNAs	miRanda	TargetScan	PicTar
dme-miR-219	+	+	+
dme-miR-277	+	+	
dme-miR-281	+		+
dme-miR-375	+	+	
dme-miR-960	+	+	
dme-miR-974	+	+	
dme-miR-976	+	+	
dme-miR-991		+	
dme-miR-1007		+	
dme-miR-1010	+	+	
dme-miR-1017		+	

+: Predicted by software.

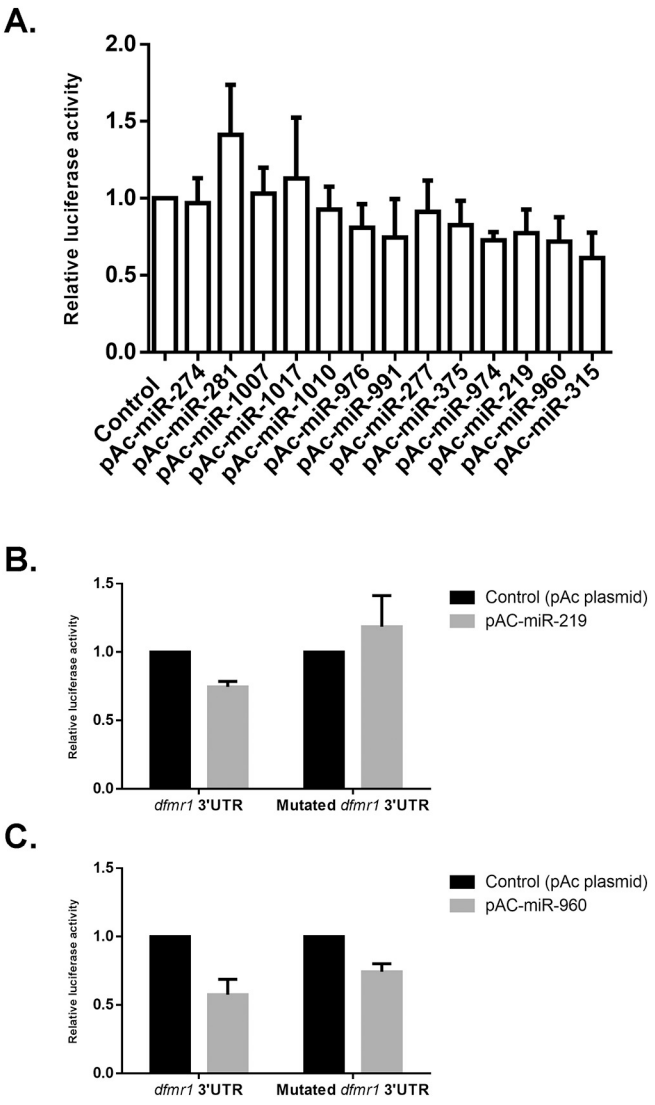

Fig. 1. Screening of candidate miRNAs in Kc167 cells.
(A) Relative values of luciferase activity with 13 miRNAs potentially acting on the 3′-UTR of the *dFMR1* transcript. MiR-274 and miR-315 were used as a negative and positive control, respectively. Blank control was set as 1. (B) Relative values of luciferase activity before and after mutation of two miR-219 binding sites of 3′-UTR of *dFMR1* transcript. $n = 5$. (C) Relative values of luciferase activity before and after mutation of the miR-960 binding site of 3′-UTR of *dFMR1* transcript. $n = 5$.

3.3. miR-219 and miR-960 interact with the 3′-UTR of the dFMR1 transcript

Based on bioinformatics analysis, two sites in miR-219 and one site in miR-960 were predicted to bind to the 3′-UTR of the *dFMR1* transcript (Table 2). We mutated these sited and conducted a luciferase activity assay in Kc167 cells. The results showed that the luciferase activity was 74.50% ± 4.05% of the empty plasmid control before and 118.51% ± 22.75% after mutation of the two miR-219 binding sites (Fig. 1B), and 57.58% ± 11.29% of the empty plasmid control before and 74.28% ± 5.94% after mutation of the miR-960 binding site. In short, when binding sites in the 3′-UTR of the *dFMR1* transcript were mutated (Fig. 1C), the luciferase activity was restored to varying

Table 2
Predicted consequential pairing of target region (top) and miRNA (bottom), and mutated sequences of target regions (small letters).

Sequence ID	Predicted consequential pairing
Position 506-512 of *dFMR1* 3′-UTR	5′...AAAAAAGCUUCAAUAACAAUCAA…
	| | | | | |
dme-miR-219	3′…UCUUAACGCAAACCUGUUAGU
Mut_1 on *dFMR1* 3′-UTR	5′…AAAAAAGCUUCAAUAgcggccgcA…
	*Not*I
Position 1346-1352 of *dFMR1* 3′-UTR	5′…AGAGGAGCAUUGAACACAAUCAU…
	| | | | | |
dme-miR-219	3′…UCUUAACGCAAACCUGUUAGU
Mut_2 on *dFMR1* 3′-UTR	5′...AGAGGAGCAUUGAACctcgagU…
	*Xho*I
Position 1286-1292 of *dFMR1* 3′-UTR	5′…CUUAGUCCUCUAUUAAAUACUCU…
	| | | | | | |
dme-miR-960	3′…CGAUACGUUAGACCUUAUGAGU
Mut_3 on *dFMR1* 3′-UTR	5′…CUUAGUCCUCUAUUAgcggccgcU…
	*Not*I

Mut_1 and Mut_2 positions were mutated simultaneously for dme-miR-219 testing.
Mut_3 position was mutated for dme-miR-960 testing.

degrees, compared to the non-mutated 3′-UTR.

3.4. Overexpression of miR-219 leads to decreased levels of dFMRP

Because dFMRP is mainly expressed in the brain and ventral nerve cord of *Drosophila*, we chose elav-Gal4 to drive the overexpression of miR-219. We extracted proteins from head discs obtained from third-instar larvae of w^{1118} wild-type (control), UAS-miR-219 (a transgenic strain in which the overexpression of miR-219 is not driven), and Elav > miR-219 (miR-219 overexpression specifically in the nervous system) *Drosophila* for western blot analysis. There was no difference in the dFMRP protein level between wild-type and UAS-miR-219 *Drosophila*. However, when miR-219 was driven by elav-Gal4, the dFMRP protein level was significantly lower than that in the wild-type (Fig. 2).

3.5. Overexpression of miR-219 leads to changes in the NMJ synaptic structure

HRP and DLG are a specific presynaptic and a specific postsynaptic marker, respectively, that we used to observe the *Drosophila* NMJ and boutons (Fig. 3A and B). We observed w^{1118}, UAS-miR-219, Elav > miR-219, and the *dfmr1* mutant (BL6930, no dFMRP expression) flies. A Kruskal-Wallis test indicated a significant difference in the number of synaptic branches among the four groups ($P < 0.0001$). Post-hoc tests indicated that Elav > miR-219 and the *dfmr1* mutant had significantly more branches than w^{1118} or UAS-miR-219 (Dunn's multiple comparisons tests: $w^{1118} = 2.739 \pm 0.7518$ [$n = 23$] vs. Elav > miR-219 = 4.387 ± 0.9193 [$n = 31$], $P < 0.0001$; $w^{1118} = 2.739 \pm 0.7518$ [$n = 23$] vs. *dfmr1* mutant = 4.625 ± 0.7440 [$n = 8$], $P < 0.001$; UAS-miR-219 = 3.154 ± 0.6887 [$n = 13$] vs. Elav > miR-219 = 4.387 ± 0.9193 [$n = 31$], $P < 0.01$; UAS-miR-219 = 3.154 ± 0.6887 [$n = 13$] vs. *dfmr1* mutant = 4.625 ± 0.7440 [$n = 8$], $P < 0.05$) (Fig. 3A and C).

Likewise, the number of synaptic boutons was significantly different among the four strains (Kruskal-Wallis test, $P < 0.0001$). Post-hoc tests revealed that Elav > miR-219 and the *dfmr1* mutant had more synaptic boutons than w^{1118} or UAS-miR-219 (Dunn's multiple comparisons tests: $w^{1118} = 17.43 \pm 1.779$ [$n = 23$] vs. Elav > miR-219 = 20.55 ± 1.767 [$n = 31$], $P < 0.0001$; $w^{1118} = 17.43 \pm 1.779$ [$n = 23$] vs. *dfmr1* mutant = 24.50 ± 1.069 [$n = 8$], $P < 0.0001$; UAS-miR-219 = 18.40 ± 1.502 [$n = 15$] vs. Elav > miR-219 = 20.55 ± 1.767 [$n = 31$], $P < 0.05$; UAS-miR-219 = 18.40 ± 1.502 [$n = 15$] vs. *dfmr1* mutant = 24.50 ± 1.069 [$n = 8$], $P < 0.0001$) (Fig. 3A and D). Both the changes in synaptic branches and in boutons were due to the decreased level of dFMRP caused by the repression of miR-219 (Fig. 3C and D). Notably, bouton numbers differed significantly between Elav > miR-219 and *dfmr1*

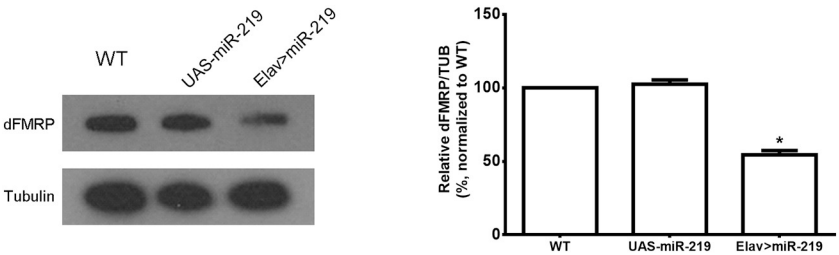

Fig. 2. Western blot analysis of dFMRP.
Western blot analysis for dFMRP protein in wild-type (WT), UAS-miR-219 transgenic line, and Elav > miR-219 (elav-Gal4-driven miR-219 overexpression) flies. Tubulin was used as a loading control. *$P < 0.05$. $n = 5$.

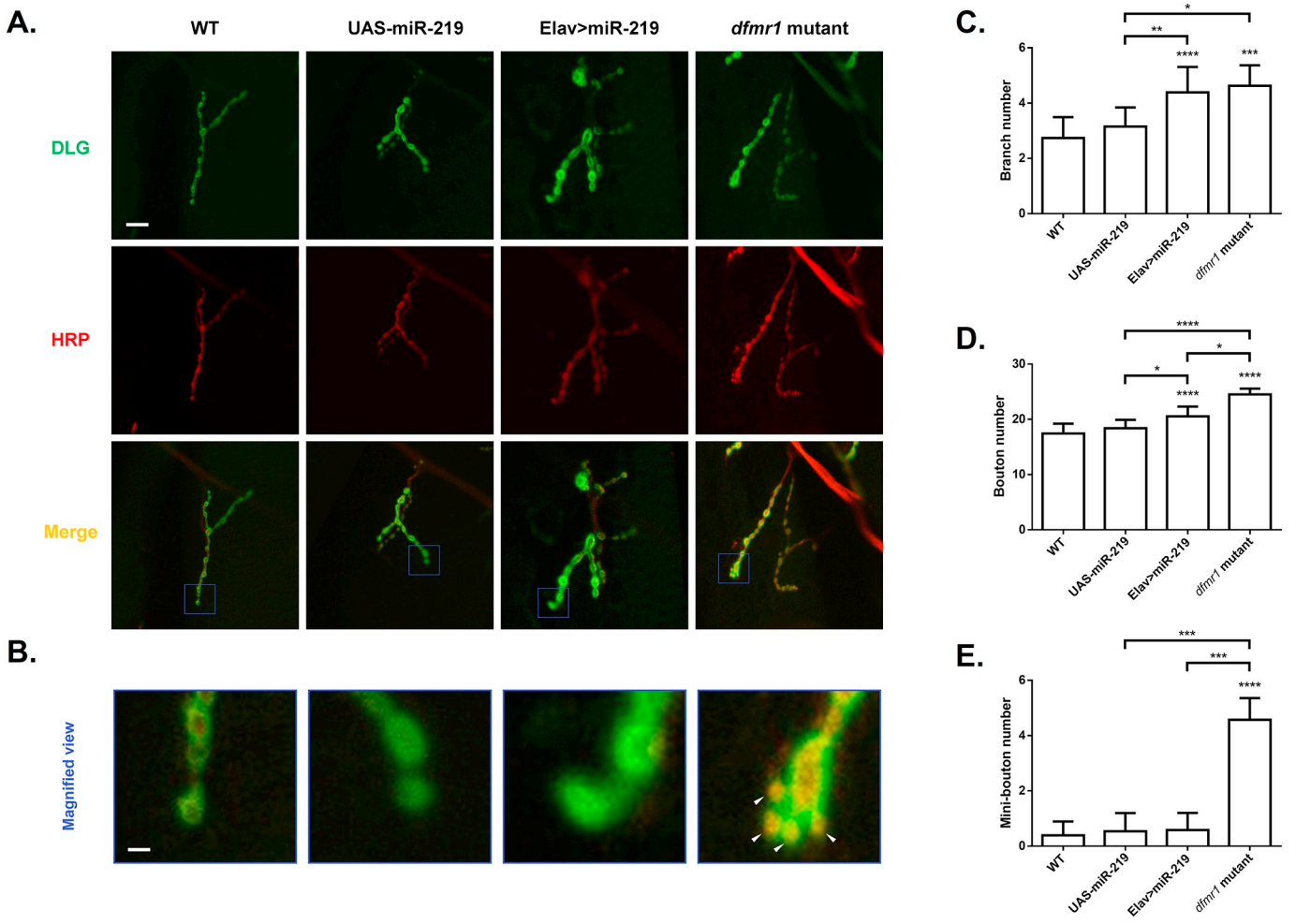

Fig. 3. NMJ staining and analysis.
(A) NMJs in wild-type (WT), UAS-miR-219 transgenic line, Elav > miR-219 (elav-Gal4-driven miR-219 overexpression), and *dfmr1* mutant flies were stained with anti-HRP (HRP) or anti-DLG (DLG). Boutons were identified on the basis of a merged image. Scale bar represents 20 μm. (B) Magnified views of areas enclosed in blue boxes in (A). Scale bar represents 4 μm. White arrowheads highlight mini-boutons. (C–E) Quantitative analysis of branch number (C), bouton number (D), and mini-bouton number (E). $^{*}P < 0.05$; $^{**}P < 0.01$; $^{***}P < 0.001$; $^{****}P < 0.0001$. (For interpretation of the references to color in this figure legend, the reader is referred to the web version of this article.)

mutant (Dunn's multiple comparisons test: Elav > miR-219 = 20.55 ± 1.767 [$n = 31$] vs. *dfmr1* mutant = 24.50 ± 1.069 [$n = 8$], $P < 0.05$) (Fig. 3D).

Finally, the numbers of mini-boutons differed significantly among the four groups (Kruskal-Wallis test, $P < 0.0001$). The *dfmr1* mutant had significantly more mini-boutons than w^{1118}, UAS-miR-219, and Elav > miR-219 (Dunn's multiple comparisons tests: w^{1118} = 0.3913 ± 0.4990 [$n = 23$] vs. *dfmr1* mutant = 4.571 ± 0.7868 [$n = 7$], $P < 0.0001$; UAS-miR-219 = 0.5385 ± 0.6602 [$n = 13$] vs. *dfmr1* mutant = 4.571 ± 0.7868 [$n = 7$], $P < 0.001$; Elav > miR-219 = 0.5806 ± 0.6204 [$n = 31$] vs. *dfmr1* mutant = 4.571 ± 0.7868 [$n = 7$], $P < 0.001$). No differences were observed between Elav > miR-219 and w^{1118} (Dunn's multiple comparisons test: w^{1118} = 0.3913 ± 0.4990 [$n = 23$] vs. Elav > miR-219 = 0.5806 ± 0.6204 [$n = 31$], $P > 0.05$) (Fig. 3B and E).

4. Discussion

The dFMRP protein consists of 684 amino acids and has a molecular weight of approximately 85 kDa. Similar to human FMRP, dFMRP has five characteristic domains, namely a nuclear export signal (NES), a nuclear localisation signal (NLS), an RGG box, and two KH homology domains. Sequence alignment indicated that dFMRP has 56% sequence identity with human FMRP, with over 80% identity at the N-terminus of the protein [18]. Therefore, studying the function of dFMRP in *Drosophila* is of significance to explore the potential function of FMRP in humans.

dFMRP is ubiquitously expressed in the central nervous system, reproductive system, and muscle tissues of *Drosophila*, but it is expressed at higher levels in the nervous system [18]. Therefore, we also considered the expression pattern of miRNA when screening the miRNAs that interact with the *dFMR1* transcript. In-situ hybridisation of the two selected miRNAs, miR-219, and miR-960, showed that they were widely expressed during embryonic development in *Drosophila*, and their expression level in the nervous system was higher in the later stages of development (Supplementary material, Fig. S1). The localization of both miRNAs largely overlapped with that of dFMRP, which provided further support of the potential interaction between miR-219 or miR-960 and *dFMR1* transcript. miR-219 is highly conserved and homologous among species, including *Drosophila* and humans [26–28]. The endogenous function of miR-219 in *Drosophila* has not been previously reported. Therefore, our findings extend the scientific

understanding of miRNAs and their target molecules, and suggest that miR-219 may be involved in regulating the FMRP level in humans and thus, the translation of other mRNAs. On the other hand, miR-960 has been identified only in the genus *Drosophila*, and no homologue has been found in other species. Therefore, we did not study its functions further.

The NMJ of *Drosophila* is a good model for studying the function of the nervous system. The NMJ, which connects nerve endings and muscles, is the most widely studied synapse structure [29–32]. It represents a typical chemical synapse, which is a hub for chemical, nutritional status, and muscle feedback signals. Such synapses are formed by a number of structural specialisations called boutons. Our study revealed that overexpression of miR-219 in *Drosophila* can effectively reduce the level of dFMRP protein (Fig. 2) and cause various structural abnormalities of the NMJ. The abnormal NMJ phenotype, including increases in the numbers of synapse branches and boutons, was similar to that of the *dfmr1* mutant (Fig. 3). On the other hand, the *dfmr1* mutant had a much more severe phenotype than flies overexpressing miR-219, especially in the numbers of boutons and mini-boutons (Fig. 3D and E), suggesting that miR-219 fine-tunes the dFMRP protein level rather than silencing dFMRP expression. MiR-219 overexpression led to increased synaptic growth, which implies that transmitter release per bouton resulting in normal muscle excitation is decreased [33–35]. In fact, irrespective of the function of FMRP in the nervous system, numerous studies have reported that miR-219 regulates nervous system function. For example, in a study of Alzheimer's disease, it was reported that miR-219 could inhibit the toxicity of overexpressed human Tau protein in a *Drosophila* model [36]. In the human brain, miR-219 is closely linked to *N*-methyl-D-aspartate (NMDA) receptor signalling. The indispensable NMDA receptor-mediated downstream response element of calcium signalling, CaMKIIγ, is a target of miR-219, and dysregulation of miR-219 expression can lead to mental illnesses such as schizophrenia [26]. Further, miR-219 promotes oligodendrocyte differentiation and maturation by repressing negative regulators of oligodendrocyte differentiation [37].

5. Conclusions

Our findings pave the way for further studies on the potential link of miR-219 with fragile X syndrome. Given the relationship between FMRP and miRNA pathways, our findings suggest that miR-219 might regulate protein translation by regulating FMRP. However, one of the limitations of our study is that we did not further evaluate miR-219-regulated FMRP mRNA expression, which will be addressed in future studies.

Supplementary data to this article can be found online at https://doi.org/10.1016/j.lfs.2018.12.008.

Funding

This study was supported by the Open Fund of State Key Laboratory of Pharmaceutical Biotechnology, Nanjing University, China (No. KF-GN-201303).

Acknowledgement

We thank Adam & Stone Bio-Medicals Ltd. Co. (Soochow, China) for language polishing.

Author contribution

C. Wang analysed data, prepared figures, and wrote the manuscript. L. Ge, J. Wu, X. Wang, and C. Wang performed experiments. L. Yuan designed the research, gave key advice, provided essential assistance, finished the paper, and provided funds for the project.

Declaration of interest

The authors declare that there are no conflicts of interest.

References

[1] C. Verheij, et al., Characterization and localization of the FMR-1 gene product associated with fragile X syndrome, Nature 363 (6431) (1993) 722–724.
[2] J.A. Suhl, S.T. Warren, Single-nucleotide mutations in FMR1 reveal novel functions and regulatory mechanisms of the fragile X syndrome protein FMRP, J. Exp. Neurosci. 9 (Suppl. 2) (2015) 35–41.
[3] L.K. Myrick, et al., Independent role for presynaptic FMRP revealed by an FMR1 missense mutation associated with intellectual disability and seizures, Proc. Natl. Acad. Sci. U. S. A. 112 (4) (2015) 949–956.
[4] G.S. Conway, Premature ovarian failure and FMR1 gene mutations: an update, Ann. Endocrinol. (Paris) 71 (3) (2010) 215–217.
[5] A. Eslami, et al., FMR1 premutation: not only important in premature ovarian failure but also in diminished ovarian reserve, Hum. Fertil. (Camb.) 20 (2) (2017) 120–125.
[6] R. Hagerman, et al., FMR1 premutation and full mutation molecular mechanisms related to autism, J. Neurodev. Disord. 3 (3) (2011) 211–224.
[7] O. Lopez-Mourelo, et al., Social anxiety and autism spectrum traits among adult FMR1 premutation carriers, Clin. Genet. 91 (1) (2017) 111–114.
[8] M.W. Kurz, et al., FMR1 alleles in Parkinson's disease: relation to cognitive decline and hallucinations, a longitudinal study, J. Geriatr. Psychiatry Neurol. 20 (2) (2007) 89–92.
[9] S.M. Till, The developmental roles of FMRP, Biochem. Soc. Trans. 38 (2) (2010) 507–510.
[10] V. Brown, et al., Purified recombinant Fmrp exhibits selective RNA binding as an intrinsic property of the fragile X mental retardation protein, J. Biol. Chem. 273 (25) (1998) 15521–15527.
[11] B. Laggerbauer, et al., Evidence that fragile X mental retardation protein is a negative regulator of translation, Hum. Mol. Genet. 10 (4) (2001) 329–338.
[12] L.N. Antar, et al., Localization of FMRP-associated mRNA granules and requirement of microtubules for activity-dependent trafficking in hippocampal neurons, Genes Brain Behav. 4 (6) (2005) 350–359.
[13] K.M. Huber, et al., Altered synaptic plasticity in a mouse model of fragile X mental retardation, Proc. Natl. Acad. Sci. U. S. A. 99 (11) (2002) 7746–7750.
[14] P. Jin, et al., RNA and microRNAs in fragile X mental retardation, Nat. Cell Biol. 6 (11) (2004) 1048–1053.
[15] Y. Yang, et al., The bantam microRNA is associated with *Drosophila* fragile X mental retardation protein and regulates the fate of germline stem cells, PLoS Genet. 5 (4) (2009) e1000444.
[16] X.L. Xu, et al., The steady-state level of the nervous-system-specific microRNA-124a is regulated by dFMR1 in *Drosophila*, J. Neurosci. 28 (46) (2008) 11883–11889.
[17] S. Zongaro, et al., The 3 UTR of FMR1 mRNA is a target of miR-101, miR-129-5p and miR-221: implications for the molecular pathology of FXTAS at the synapse, Hum. Mol. Genet. 22 (10) (2013) 1971–1982.
[18] L. Wan, et al., Characterization of dFMR1, a *Drosophila melanogaster* homolog of the fragile X mental retardation protein, Mol. Cell. Biol. 20 (22) (2000) 8536–8547.
[19] A.J. Enright, et al., MicroRNA targets in *Drosophila*, Genome Biol. 5 (1) (2003) R1.
[20] B.P. Lewis, et al., Prediction of mammalian microRNA targets, Cell 115 (7) (2003) 787–798.
[21] A. Krek, et al., Combinatorial microRNA target predictions, Nat. Genet. 37 (5) (2005) 495–500.
[22] M. O'Connor, W. Chia, P element-mediated germ-line transformation of *Drosophila*, Methods Mol. Biol. 18 (1993) 75–85.
[23] A.A. Szekely, et al., P element mediated germ line transformation of *Drosophila melanogaster* with the Tc1 transposable DNA element from *Caenorhabditis elegans*, Genome 37 (3) (1994) 356–366.
[24] J. Kaur, A.K. Bachhawat, A modified Western blot protocol for enhanced sensitivity in the detection of a membrane protein, Anal. Biochem. 384 (2) (2009) 348–349.
[25] Y.Q. Zhang, et al., Drosophila fragile X-related gene regulates the MAP1B homolog Futsch to control synaptic structure and function, Cell 107 (5) (2001) 591–603.
[26] J. Kocerha, et al., MicroRNA-219 modulates NMDA receptor-mediated neurobehavioral dysfunction, Proc. Natl. Acad. Sci. U. S. A. 106 (9) (2009) 3507–3512.
[27] H.Y. Cheng, et al., microRNA modulation of circadian-clock period and entrainment, Neuron 54 (5) (2007) 813–829.
[28] W.J. Lukiw, Micro-RNA speciation in fetal, adult and Alzheimer's disease hippocampus, Neuroreport 18 (3) (2007) 297–300.
[29] C.R. Slater, et al., Pre- and post-synaptic abnormalities associated with impaired neuromuscular transmission in a group of patients with 'limb-girdle myasthenia', Brain 129 (Pt 8) (2006) 2061–2076.
[30] Y.C. Chen, et al., *Drosophila* neuroligin 2 is required presynaptically and postsynaptically for proper synaptic differentiation and synaptic transmission, J. Neurosci. 32 (45) (2012) 16018–16030.
[31] S. Lee, et al., Phospho-dependent ubiquitination and degradation of PAR-1 regulates

synaptic morphology and tau-mediated Abeta toxicity in *Drosophila*, Nat. Commun. 3 (2012) 1312.
[32] Y. Jin, Synaptogenesis: insights from worm and fly, Curr. Opin. Neurobiol. 12 (1) (2002) 71–79.
[33] G.W. Davis, C.S. Goodman, Genetic analysis of synaptic development and plasticity: homeostatic regulation of synaptic efficacy, Curr. Opin. Neurobiol. 8 (1) (1998) 149–156.
[34] C.M. Schuster, et al., Genetic dissection of structural and functional components of synaptic plasticity. II. Fasciclin II controls presynaptic structural plasticity, Neuron 17 (4) (1996) 655–667.
[35] C.M. Schuster, et al., Genetic dissection of structural and functional components of synaptic plasticity. I. Fasciclin II controls synaptic stabilization and growth, Neuron 17 (4) (1996) 641–654.
[36] I. Santa-Maria, et al., Dysregulation of microRNA-219 promotes neurodegeneration through post-transcriptional regulation of tau, J. Clin. Invest. 125 (2) (2015) 681–686.
[37] X. Zhao, et al., MicroRNA-mediated control of oligodendrocyte differentiation, Neuron 65 (5) (2010) 612–626.